

# High-order Linearly Energy-preserving Compact Finite Difference Schemes for the Korteweg-de Vries Equation

Jin-Liang Yan and Liang-Hong Zheng and Fu-Qiang Lu and Wen-Jun Li

**Abstract**—In this paper, the discrete variational derivative method (DVDM) and the compact difference method are combined to construct linearly energy-preserving schemes for the Korteweg-de Vries equation. The sixth-order compact difference method is used in the spatial direction, and the discrete variational derivative method is used in the temporal direction. The resulting fully discrete schemes are linear, unconditionally stable, uniquely solvable, and can precisely conserve the discrete mass and energy. At last, some benchmark numerical examples are given to demonstrate the accuracy and efficiency of the proposed schemes. Numerical results show that the proposed schemes are more advantageous than the existing methods.

**Index Terms**—Energy; Compact difference scheme; DVDM; Korteweg-de Vries equation

## I. INTRODUCTION

THE Korteweg-de Vries (KdV) equation

$$\frac{\partial u}{\partial t} + \varepsilon u \frac{\partial u}{\partial x} + \mu \frac{\partial^3 u}{\partial x^3} = 0, \quad (1)$$

describes the evolution of the solitary wave. The parameters  $\varepsilon$ ,  $\mu$  represent real constants. To determine the solution of (1), we prescribe the following initial value and periodic boundary condition

$$u(x, 0) = u_0(x), \quad u(a, t) = u(b, t).$$

The KdV equation is a completely integrable equation, it has infinite number of conserved properties [1], the first three conservation laws are

$$\begin{aligned} \mathcal{M}(t) &= \int_a^b u \, dx, \\ \mathcal{K}(t) &= \frac{1}{2} \int_a^b u^2 \, dx, \\ \mathcal{H}(t) &= \int_a^b \left[ -\frac{\varepsilon}{6} u^3 + \frac{\mu}{2} u_x^2 \right] dx, \end{aligned}$$

Manuscript received September 27, 2021; revised March 21, 2022. This work was supported in part by the National Natural Science of China (Grant No. 11861047, 41901323, 11971241), Natural Science Foundation of Fujian Province (Grant No. 2019J01831), Foundation Jiangsu Key Laboratory for NSLSCS (Grant No. 201804), PhD Start-up Fund of Wuyi University (Grant No. YJ201702), Teacher and Student Scientific Team Fund of Wuyi University (Grant No. 2020-SSTD-003).

Jin-Liang Yan is an associate professor of Mathematics and Computer Department, Wuyi University, Wuyi Shan, Fujian, 354300, China. (e-mail: yanjinliang3333@163.com).

Liang-Hong Zheng is a lecturer of Information and Computer Technology Department, No. 1 middle school of Nanping, Nanping, Fujian, 353000, China. (e-mail: 413845939@qq.com).

Fu-Qiang Lu is a lecturer of Changzhou Institute of Technology, Changzhou, 213032, China. (e-mail: 724075305@qq.com).

Wen-Jun Li is an undergraduate student of Mathematics and Computer Department, Wuyi University, Wuyi Shan, Fujian, 354300, China. (e-mail: 1395418838@qq.com).

which are respectively named mass, momentum and energy.

The quality of a numerical approximation hinges on how well the physical properties of the original system can be preserved. The conservative methods have been shown to enjoy favorable properties such as qualitative solution behavior and improved overall accuracy [2]. To our knowledge, there have been many results for the KdV equation. For instance, finite difference methods [3], [4], finite element methods [5], [6], spectral method [7] and operator splitting method [8], and so on. However, the majority of the aforementioned methods are designed to preserve only  $\mathcal{M}$ , not other invariants.

Besides, some other methods are proposed to conserve the invariants of the KdV equation. For example, symplectic methods [9], [10], momentum-preserving methods [11]–[13], and energy-preserving methods [14]–[16]. It is worthwhile to note that Gong [10] proposed several systematic methods to discretize general multi-symplectic formulations of the Hamiltonian partial differential equations (PDEs). Yi [11], Bona [12] and Yan [13] designed some momentum-preserving schemes to solve the KdV equation. More recently, researchers paid more attention to the energy-preserving methods, for example, Celledoni proposed an average vector field (AVF) method in [14], Brugnano [15] developed the Hamiltonian boundary value method (HBVM) and Furihata [16] proposed the discrete variational derivative method (DVDM) to solve the general conservative or dissipative PDEs. The DVDM methods has been extended in various aspects. For more details see [17]–[20]. Inspired by the compact DVDM in [19], we designed two linearly energy-preserving schemes to solve the KdV equation.

The rest of this paper is organized as follows. In Section 2, we briefly introduce the basic knowledge of the compact difference method, and derive the proposed energy-preserving schemes. In Section 3, the uniqueness and solvability of the proposed schemes are analyzed. In Section 4, we analyze the linear stability of the proposed schemes. In Section 5, some numerical examples are presented to validate the efficiency of the proposed schemes. At last, some conclusions are given.

## II. LINEARLY ENERGY-PRESERVING SCHEMES

The equation (1) can be rewritten as the following Hamiltonian form

$$u_t = \frac{\partial}{\partial x} \left( \frac{\delta G}{\delta u} \right), \quad G(u, u_x) = -\frac{\varepsilon}{6} u^3 + \frac{\mu}{2} u_x^2 \quad (2)$$

where  $G(u, u_x)$  represents local energy, and  $\frac{\delta G}{\delta u}$  denotes the variational derivative of  $G$  with respect to  $u$ , i.e.  $\frac{\delta G}{\delta u} = \frac{\partial G}{\partial u} - \frac{\partial}{\partial x} \left( \frac{\partial G}{\partial u_x} \right)$ .

A. Compact finite difference method

Firstly, we briefly describe the framework of compact difference method. For more details refer to see [19], [21], [22] and references therein.

Given a sufficiently smooth function  $f(x)$ , which is approximated by  $f_i$  ( $i = 0, 1, \dots, N - 1$ ) on the uniform mesh with the mesh size  $h = (b - a)/N$ . In the following, unless otherwise specified, the discrete periodic boundary conditions  $f_{i \pm N} = f_i$  will be supposed and the values for the nodes outside  $i = 0, 1, \dots, N$  will be periodically defined.

Typical compact finite difference operator for  $\partial/\partial x$  is defined in the following form

$$f'_j + \alpha (f'_{j+1} + f'_{j-1}) + \beta (f'_{j+2} + f'_{j-2}) = a \frac{f_{j+1} - f_{j-1}}{2h} + b \frac{f_{j+2} - f_{j-2}}{4h} + c \frac{f_{j+3} - f_{j-3}}{6h}, \quad (3)$$

where  $\alpha, \beta, a, b,$  and  $c$  are real constants.

Equality (3) can also be expressed in the following matrix form

$$Tf' = Sf, \quad (4)$$

where

$$f = (f_1, f_2, \dots, f_N)^T, \quad f' = (f'_1, f'_2, \dots, f'_N)^T, \\ T = C(1, \alpha, \beta, 0, \dots, 0, \beta, \alpha), \\ S = \frac{1}{12h}C(0, 6a, 3b, 2c, 0, \dots, 0, -2c, -3b, -6a),$$

wherein  $T$  and  $S$  are respectively  $N \times N$  symmetric and anti-symmetric matrix.

In particular, when  $\alpha = \beta = 0, a = \frac{3}{2}, b = -\frac{3}{5}, c = \frac{1}{10}$  and  $\alpha = \frac{1}{3}, \beta = 0, a = \frac{14}{9}, b = \frac{1}{9}, c = 0$ , the sixth order (i.e.  $O(h^6)$ ) standard central finite difference operator (C6) and a three point compact difference operator (T6) are respectively obtained for  $\partial/\partial x$ .

**Proposition II.1.** Let  $h > 0, f(x) \in C^7[a, b]$  and  $\alpha = \frac{1}{3}, \beta = 0, a = \frac{14}{9}, b = \frac{1}{9}$  and  $c = 0$ , the truncation error of the compact difference operator (T6) is  $-\frac{1}{1260}f_j^{(7)}h^6$ .

*Proof:* By resorting to the Taylor formula, expanding the left side of (3) at node  $x = x_j, j = 0, 1, \dots, N$ , we have

$$f'_j = f'_j, \\ \alpha f'_{j-1} = \alpha f'_j - \alpha h f''_j + \alpha \frac{h^2}{2} f_j^{(3)} - \alpha \frac{h^3}{6} f_j^{(4)} + \alpha \frac{h^4}{24} f_j^{(5)} - \alpha \frac{h^5}{120} f_j^{(6)} + \alpha \frac{h^6}{720} f_j^{(7)} - \frac{h^7}{5040} f_j^{(8)} + O(h^7), \\ \alpha f'_{j+1} = \alpha f'_j + \alpha h f''_j + \alpha \frac{h^2}{2} f_j^{(3)} + \alpha \frac{h^3}{6} f_j^{(4)} + \alpha \frac{h^4}{24} f_j^{(5)} + \alpha \frac{h^5}{120} f_j^{(6)} + \alpha \frac{h^6}{720} f_j^{(7)} + \frac{h^7}{5040} f_j^{(8)} + O(h^7).$$

Adding up both sides of the above equalities, we get

$$\alpha f'_{j-1} + f'_j + \alpha f'_{j+1} = (2\alpha + 1) f'_j + \alpha h^2 f_j^{(3)} + \alpha \frac{h^4}{12} f_j^{(5)} + \alpha \frac{h^6}{360} f_j^{(7)} + O(h^7). \quad (5)$$

Next, expanding the right side of (3) at node  $x = x_j, j = 0, 1, \dots, N$ , we have

$$b \frac{f_{j+2} - f_{j-2}}{4h} = b f'_j + \frac{4}{6} b h^2 f_j^{(3)} + \frac{16}{120} b h^4 f_j^{(5)} + \frac{64}{5040} b h^6 f_j^{(7)} + O(h^7).$$

$$a \frac{f_{j+1} - f_{j-1}}{2h} = a f'_j + \frac{1}{6} a h^2 f_j^{(3)} + \frac{1}{120} a h^4 f_j^{(5)} + \frac{1}{5040} a h^6 f_j^{(7)} + O(h^7).$$

Adding up both sides of the above equalities, we have

$$b \frac{f_{j+2} - f_{j-2}}{4h} + a \frac{f_{j+1} - f_{j-1}}{2h} = (a + b) f'_j + \frac{(a + 2^2 b)}{6} h^2 f_j^{(3)} + \frac{(a + 2^4 b)}{120} h^4 f_j^{(5)} + \frac{(a + 2^6 b)}{5040} h^6 f_j^{(7)} + O(h^7). \quad (6)$$

Substituting  $\alpha = \frac{1}{3}, \beta = 0, a = \frac{14}{9}, b = \frac{1}{9},$  and  $c = 0$  into (5) and (6), we have

$$\frac{1}{3} f'_{j-1} + f'_j + \frac{1}{3} f'_{j+1} = \frac{5}{3} f'_j + \frac{1}{3} h^2 f_j^{(3)} + \frac{h^4}{36} f_j^{(5)} + \frac{h^6}{1080} f_j^{(7)} + O(h^7),$$

$$\frac{f_{j+2} - f_{j-2}}{36h} + 7 \frac{f_{j+1} - f_{j-1}}{9h} = \frac{5}{3} f'_j + \frac{1}{3} h^2 f_j^{(3)} + \frac{1}{36h} h^4 f_j^{(5)} + \frac{13}{7560} h^6 f_j^{(7)} + O(h^7).$$

Subtracting the above two equations, we have

$$\frac{1}{3} f'_{j-1} + f'_j + \frac{1}{3} f'_{j+1} - \frac{1}{36h} (f_{j+2} - f_{j-2}) - \frac{7}{9h} (f_{j+1} - f_{j-1}) = -\frac{1}{1260} f_j^{(7)} h^6.$$

Thus, the result is hold. ■

Similarly, the compact difference operator for  $\partial^2/\partial x^2$  is defined in the following form

$$f''_j + \hat{\alpha} (f''_{j+1} + f''_{j-1}) + \hat{\beta} (f''_{j+2} + f''_{j-2}) = \hat{a} \frac{f_{j+1} - 2f_j + f_{j-1}}{h^2} + \hat{b} \frac{f_{j+2} - 2f_j + f_{j-2}}{4h^2} + \hat{c} \frac{f_{j+3} - 2f_j + f_{j-3}}{9h^2}, \quad (7)$$

where  $\hat{\alpha}, \hat{\beta}, \hat{a}, \hat{b}$  and  $\hat{c}$  are real constants.

Denote  $\hat{d} = -72\hat{\alpha} + 18\hat{b} + 8\hat{c}$ , equality (7) can also be expressed in the following matrix form

$$T_1 f'' = S_1 f,$$

where

$$f = (f_1, f_2, \dots, f_N)^T, \quad f'' = (f''_1, f''_2, \dots, f''_N)^T, \\ T_1 = C(1, \alpha, \beta, 0, \dots, 0, \beta, \alpha), \\ S_1 = (1/36h^2)C(\hat{d}, 36\hat{a}, 9\hat{b}, 4\hat{c}, 0, \dots, 0, 4\hat{c}, 9\hat{b}, 36\hat{a}).$$

wherein  $T_1$  and  $S_1$  are respectively  $N \times N$  symmetric circulant matrix.

In particular, in case of  $\hat{\alpha} = \hat{\beta} = 0, \hat{a} = \frac{3}{2}, \hat{b} = -\frac{3}{5}, \hat{c} = \frac{1}{10}$  and  $\hat{\alpha} = \frac{2}{11}, \hat{\beta} = 0, \hat{a} = \frac{12}{11}, \hat{b} = \frac{3}{11}, \hat{c} = 0$ , the sixth order (i.e.  $O(h^6)$ ) standard central finite difference operator (C6) and a three point compact difference operator (T6) are respectively obtained for  $\partial^2/\partial x^2$ .

**Proposition II.2.** Let  $h > 0, f(x) \in C^7[a, b]$ , and  $\hat{\alpha} = \frac{2}{11}, \hat{\beta} = 0, \hat{a} = \frac{12}{11}, \hat{b} = \frac{3}{11}$  and  $\hat{c} = 0$ , the truncation error of the compact difference operator (T6) is  $-\frac{1}{1980}f_j^{(8)}h^6$ .

*Proof:* The proof is similar as the Proposition II.1. ■

## B. Scheme 1

Define a discrete local energy as follows

$$G_d(U^{m+1}, U^m)_i = \frac{\mu (\delta_c^{(1)} U_i^{m+1})^2 + (\delta_c^{(1)} U_i^m)^2}{2} - \frac{\varepsilon (U_i^m)^2 U_i^{m+1} + (U_i^{m+1})^2 U_i^m}{6} \quad (8)$$

where  $\delta_c^{(1)}$  denotes the first order compact difference operator.

Substituting (8) into the following equality, we have

$$\begin{aligned} & \sum_{i=0}^{N-1} \left[ G_d(U^{m+1}, U^m)_i - G_d(U^m, U^{m-1})_i \right] \Delta x \\ &= \sum_{i=0}^{N-1} \left[ -\frac{\varepsilon}{6} (U_i^m)^2 + U_i^m (U_i^{m+1} + U_i^{m-1}) \right. \\ & \quad \left. - \frac{\mu}{2} (\delta_c^{(1)})^2 (U_i^{m+1} + U_i^{m-1}) \right] \frac{U_i^{m+1} - U_i^{m-1}}{2} \Delta x \\ &= \sum_{i=0}^{N-1} \left[ -\frac{\varepsilon}{6} U_i^m (U_i^m + U_i^{m+1} + U_i^{m-1}) \right. \\ & \quad \left. - \frac{\mu}{2} (\delta_c^{(1)})^2 (U_i^{m+1} + U_i^{m-1}) \right] \frac{U_i^{m+1} - U_i^{m-1}}{2} \Delta x, \end{aligned}$$

where  $\sum_{i=0}^{N-1} f_i \triangleq \frac{1}{2} f_0 + f_1 + \dots + f_{N-1} + \frac{1}{2} f_N$  denotes the trapezoidal rule.

Then, we obtain a discrete scheme of  $\frac{\delta G}{\delta u}$  as follows,

$$\begin{aligned} \frac{\delta G_d}{\delta U_i} &= \frac{\delta G_d}{\delta (U^{m+1}, U^m, U^{m-1})_i} \\ &= -\frac{\varepsilon}{6} U_i^m (U_i^m + U_i^{m+1} + U_i^{m-1}) \\ & \quad - \frac{\mu}{2} (\delta_c^{(1)})^2 (U_i^{m+1} + U_i^{m-1}). \end{aligned} \quad (9)$$

Substituting (9) into (2) and approximating  $(u_t)_i$  by  $(U_i^{(m+1)} - U_i^{(m-1)})/2\tau$ , we have

$$\begin{aligned} \frac{U_i^{m+1} - U_i^{m-1}}{2\tau} &= -\frac{\mu}{2} \delta_c^{(1)} (\delta_c^{(1)})^2 (U_i^{m+1} + U_i^{m-1}) \\ & \quad - \frac{\varepsilon}{6} \delta_c^{(1)} U_i^m (U_i^m + U_i^{m+1} + U_i^{m-1}), \end{aligned} \quad (10)$$

where  $i = 0, 1, \dots, N$ .

Scheme 1 can also be reformulated as the following matrix form

$$\begin{aligned} (T^3 + \mu\tau S^3)U^{m+1} &= (T^3 - \mu\tau S^3)U^{m-1} \\ & \quad - \frac{\varepsilon}{3}\tau T^2 S U^m (U^{m+1} + U^m + U^{m-1}), \end{aligned} \quad (11)$$

which satisfies the following conservative properties

**Theorem II.1.** Let  $U^m$  be numerical solution of (10), and suppose it satisfies the periodic boundary conditions, then the solution of the scheme 1 (10) satisfies

$$\begin{aligned} M_d(U^{m+1}, U^m) &= M_d(U^1, U^0), \\ H_d(U^{m+1}, U^m) &= H_d(U^1, U^0). \end{aligned}$$

Proof:

$$\begin{aligned} & \frac{M_d(U^{m+1}, U^m) - M_d(U^m, U^{m-1})}{2\Delta t} \\ &= \sum_{i=0}^{N-1} \left[ \frac{U_i^{m+1} - U_i^{m-1}}{2\Delta t} \right] \Delta x \\ &= \sum_{i=0}^{N-1} \delta_c^{(1)} \frac{\delta G_d}{\delta (U^{m+1}, U^m, U^{m-1})_i} \Delta x \\ &= \left[ \frac{\delta G_d}{\delta (U^{m+1}, U^m, U^{m-1})_i} \right]_a^b = 0. \end{aligned}$$

Similarly,

$$\begin{aligned} & \frac{H_d(U^{m+1}, U^m) - H_d(U^m, U^{m-1})}{2\tau} \\ &= \sum_{i=0}^{N-1} \left[ \frac{\delta G_d}{\delta U_i} \frac{U_i^{m+1} - U_i^{m-1}}{2\tau} \right] \Delta x \\ &= \sum_{i=0}^{N-1} \left[ \frac{\delta G_d}{\delta U_i} \delta_c^{(1)} \frac{\delta G_d}{\delta U_i} \right] \Delta x \\ &= -\sum_{i=0}^{N-1} \left[ \delta_c^{(1)} \frac{\delta G_d}{\delta U_i} \frac{\delta G_d}{\delta U_i} \right] \Delta x \\ &= 0. \end{aligned}$$

■

## C. Scheme 2

Given the discrete local energy is defined as follows,

$$\begin{aligned} G_d(U^{m+1}, U^m)_i &= -\frac{\varepsilon (U_i^m)^2 U_i^{m+1} + (U_i^{m+1})^2 U_i^m}{6} \\ & \quad + \frac{\mu (\delta_c^+ U_i^{(m+1)})^2 + (\delta_c^- U_i^{(m+1)})^2}{4} \\ & \quad + \frac{\mu (\delta_c^+ U_i^m)^2 + (\delta_c^- U_i^m)^2}{4}, \end{aligned} \quad (12)$$

where  $\delta_c^+$  and  $\delta_c^-$  respectively represents the forward and backward compact difference operator.

Substituting (12) into the following equality, we have

$$\begin{aligned} & \sum_{i=0}^{N-1} \left[ G_d(U^{m+1}, U^m)_i - G_d(U^m, U^{m-1})_i \right] \Delta x \\ &= \sum_{i=0}^{N-1} \left[ -\frac{\varepsilon (U_i^m)^2 (U_i^{m+1} - U_i^{m-1})}{6} \right. \\ & \quad - \frac{\varepsilon}{12} U_i^m (U_i^{m+1} - U_i^{m-1}) (U_i^{m+1} + U_i^{m-1}) \\ & \quad - \frac{\mu}{8} \delta_c^+ (U_k^{m+1} + U_k^{m-1}) \delta_c^+ (U_k^{m+1} - U_k^{m-1}) \\ & \quad \left. - \frac{\mu}{8} \delta_c^- (U_k^{m+1} + U_k^{m-1}) \delta_c^- (U_k^{m+1} - U_k^{m-1}) \right] \Delta x \\ &= \sum_{i=0}^{N-1} \left[ -\frac{\varepsilon}{6} U_i^m (U_i^m + U_i^{m+1} + U_i^{m-1}) \right. \\ & \quad \left. - \frac{\mu}{2} \delta_c^{(2)} (U_i^{m+1} + U_i^{m-1}) \right] \frac{U_i^{m+1} - U_i^{m-1}}{2} \Delta x. \end{aligned}$$

Then, we obtain a discrete scheme of  $\frac{\delta G}{\delta u}$  as follows,

$$\frac{\delta G_d}{\delta(U_i^{m+1}, U_i^m, U_i^{m-1})_i} = -\frac{\mu}{2}\delta_c^{(2)}(U_i^{m+1} + U_i^{m-1}) - \frac{\varepsilon}{6}U_i^m(U_i^m + U_i^{m+1} + U_i^{m-1}). \quad (13)$$

Substituting (13) into (2), and approximating  $(u_t)_i$  by  $(U_i^{m+1} - U_i^{m-1})/2\Delta t$ , we have

$$\frac{U_i^{m+1} - U_i^{m-1}}{2\tau} = -\frac{\mu}{2}\delta_c^{(1)}\delta_c^{(2)}(U_i^{m+1} + U_i^{m-1}) - \frac{\varepsilon}{6}\delta_c^{(1)}U_i^m(U_i^m + U_i^{m+1} + U_i^{m-1}), \quad (14)$$

where  $i = 0, 1, \dots, N$ .

The above scheme can also be reformulated as the following matrix form

$$(TT_1 + \mu\tau SS_1)U^{m+1} = (TT_1 - \mu\tau SS_1)U^{m-1} - \frac{\varepsilon}{3}\tau T_1 S U^m (U^{m+1} + U^m + U^{m-1}),$$

which satisfies the following conservative properties,

**Theorem II.2.** *Let  $U^m$  be the solution of (14), and suppose it satisfies the periodic boundary conditions, then the solution of the scheme 2 (14) satisfies*

$$M_d(U^{m+1}, U^m) = M_d(U^1, U^0), \\ H_d(U^{m+1}, U^m) = H_d(U^1, U^0).$$

*Proof:* The proof is similar as the Theorem II.1. ■

### III. UNIQUENESS AND SOLVABILITY

**Theorem III.1.** *The Scheme 1 (10) and the Scheme 2 (14) are uniquely solvable.*

*Proof:* The Scheme 1 (11) can be written as the following matrix form

$$\mathbb{B}U^{m+1} = \mathbf{b},$$

where  $\mathbb{B} = T^3 + \mu\tau S^3 + \frac{\varepsilon}{3}\tau T^2 S \text{diag}(U^m)$  and

$$\mathbf{b} = (T^3 - \mu\tau S^3 - \frac{\varepsilon}{3}\tau T^2 S \text{diag}(U^m))U^{m-1} - \frac{\varepsilon}{3}\tau T^2 S \text{diag}(U^m)U^m.$$

In order to obtain the unique solvability of the Scheme 1, we only need to prove that  $\mathbb{B}$  is invertible.

If  $\mathbb{B}\mathbf{x} = 0$ , then

$$0 = \mathbf{x}^T \mathbb{B}\mathbf{x} = \mathbf{x}^T T^3 \mathbf{x},$$

where the skew-symmetry of  $\mu\tau S^3 + \frac{\varepsilon}{3}\tau T^2 S \text{diag}(U^m)$  was used. Note that  $T^3$  is a symmetric positive definite, thus  $\mathbf{x} = 0$ , i.e.  $\mathbb{B}\mathbf{x} = 0$  only has zero solution. Therefore,  $\mathbb{B}$  is an invertible matrix. Thus, the Scheme 1 is uniquely solvable.

Similarly, we can also prove that the scheme 2 (14) is uniquely solvable. ■

### IV. LINEAR STABILITY ANALYSIS

In this section, we will investigate the linear stability of the proposed schemes. To this end, we consider the following linear KdV equation

$$u_t + u_x + u_{xxx} = 0. \quad (15)$$

**Theorem IV.1.** *The scheme 1 (10) and the scheme 2 (14) are unconditionally linearly stable when  $\tau$  is sufficiently small.*

*Proof:* Firstly, we can easily derive the following scheme for the equation (15),

$$\frac{U_i^{m+1} - U_i^{m-1}}{2\tau} = -\delta_c^{(1)}U_i^m - \frac{1}{2}(\delta_c^{(1)})^3(U_i^{m+1} + U_i^{m-1}), \quad (16)$$

where  $i = 0, 1, \dots, N$ .

The above scheme can be reformulated as the following matrix form

$$\frac{U^{m+1} - U^{m-1}}{2\tau} = -JU^m - J^3 \frac{U^{m+1} + U^{m-1}}{2}, \quad (17)$$

where  $J = T^{-1}S$ .  $T$  is an invertible symmetric matrix and  $S$  is a skew-symmetric matrix.

Assume  $U^m$  be the exact solution of (16) and  $\hat{U}^m$  be the numerical solution of the following algorithm,

$$\frac{\hat{U}^{m+1} - \hat{U}^{m-1}}{2\tau} = -J\hat{U}^m - J^3 \frac{\hat{U}^{m+1} + \hat{U}^{m-1}}{2}. \quad (18)$$

Let  $\rho^m = \hat{U}^m - U^m$ . Subtracting (16) from (18), we obtain the following perturbation error equation:

$$\frac{\rho^{m+1} - \rho^{m-1}}{2\tau} = -J\rho^m - J^3 \frac{\rho^{m+1} + \rho^{m-1}}{2}.$$

Thus, we have

$$\begin{aligned} & (\rho^{m+1})^T \rho^{m+1} - (\rho^{m-1})^T \rho^{m-1} \\ &= (\rho^{m+1} + \rho^{m-1})^T (\rho^{m+1} - \rho^{m-1}) \\ &= -2\tau(\rho^{m+1} + \rho^{m-1})^T J \rho^m \\ &= -\tau(\rho^{m+1} + \rho^{m-1})^T J^3 (\rho^{m+1} + \rho^{m-1}) \\ &= -2\tau(\rho^{m+1} + \rho^{m-1})^T J(\bar{\rho}^m + o(\tau^2)) \\ &= -\tau(\rho^{m+1} + \rho^{m-1})^T J(\rho^{m+1} + \rho^{m-1} + o(\tau^2)), \end{aligned}$$

where  $\bar{\rho}^m = (\rho^{m+1} + \rho^{m-1})/2$ , and the skew-symmetry of  $J$  and  $J^3$  were used in the last two equalities.

Thus, when  $\tau$  is sufficiently small,

$$(\rho^{m+1})^T \rho^{m+1} - (\rho^{m-1})^T \rho^{m-1} = 0,$$

i.e., the scheme 1 (10) is unconditionally linearly stable.

Similarly, we can also prove that the scheme 2 (14) is unconditionally linearly stable. ■

### V. NUMERICAL EXPERIMENTS

In this section, some examples are presented to validate the efficiency of the proposed schemes. To this end, the  $L_\infty$  and  $L_2$  error norms and convergence order at  $t = n\tau$  are defined as

$$L_\infty = \max_{0 \leq k \leq N} |U_k^n - u(x_k, n\tau)|,$$

$$L_2 = \sum_{k=0}^N (|U_k^n - u(x_k, n\tau)|^2 h)^{1/2},$$

$$\text{order} = \log_2(\|U_{2h} - u\| / \|U_h - u\|).$$

The discrete invariants at  $t = n\tau$  are defined as

$$M_d^n = \frac{1}{2} \sum_{i=0}^{N-1} (U_i^n + U_i^{n+1}) \Delta x,$$

$$K_d^n = \frac{1}{2} \sum_{i=0}^{N-1} (U_i^n)^2 \Delta x,$$

$$H_d^n = \sum_{i=0}^{N-1} G_d(U^n, U^{n+1}) \Delta x.$$

The relative errors of the invariants on the  $n$ -th time level are computed by  $|I^n - I^0|/|I^0|$ .

### A. Single solitary wave

In this example, we adopt  $\varepsilon = 1$ ,  $\mu = 1$  and choose the following exact solution

$$u(x, t) = A \operatorname{sech}^2(\kappa(x - ct - x_0)),$$

where  $A = 3c$ ,  $\kappa = \sqrt{c}/2\mu$ , and  $c$  denotes the speed of the wave.

In this example, we mainly consider the following tests:

(i) The accuracy of the proposed schemes. Here, we choose  $x_0 = 0$ ,  $c = 1$ , and  $-40 \leq x \leq 40$ . To check the accuracy of the proposed schemes in the spatial direction, we chose a relatively small time step  $\tau = 1 \times 10^{-6}$ , so that the error from the temporal direction can be negligible. Table I and Table II respectively presents the spatial errors and convergence rates of the proposed schemes. It is clearly seen that the Scheme 1 and Scheme 2 can reach sixth-order accuracy in space. Similarly, to measure the accuracy of the proposed schemes in the temporal direction, the spatial step is chosen as  $h = 1/16$ , and the temporal steps are respectively chosen as  $\tau = 1/5, 1/10, 1/20, 1/40$ . The results are listed in Table II, which indicates that the Scheme 1 is second-order accuracy in time.

(ii) The conservative properties and long time behaviors of the proposed schemes. To this end, set  $x_0 = 0$ ,  $c = 1$ , and mesh sizes are respectively taken as  $h = 0.1$ ,  $\tau = 0.01$ , and computation domain is chosen as  $[-20, 20]$ . Figure 1 presents the numerical results of the Scheme 1 over  $t \in [0, 5]$ . As is shown in the Figure 1(b), the Scheme 1 can precisely conserve the discrete mass and energy, and approximately conserve the discrete momentum to  $10^{-8}$ . Figure 2 presents the numerical results of the Scheme 1 over  $t \in [0, 200]$ . It shows that the Scheme 1 still can precisely conserve the discrete mass and energy after long time computation. The results of the Scheme 2 are similar to the Scheme 1, for simplicity, we do not list it again.

### B. Interaction of two solitary waves

In this example, we study the interaction of two solitary waves with different amplitudes and traveling in the same direction. The KdV equation (1) has the following exact solution,

$$u(x, t) = 12 \frac{F(x, t)}{G(x, t)}, \quad x \in [0, 4], \quad t \in [0, 6],$$

$$F(x, t) = k_1^2 e^{\theta_1} + k_2^2 e^{\theta_2} + 2(k_2 - k_1) e^{\theta_1 + \theta_2}$$

$$+ a^2 (k_2^2 e^{\theta_1} + k_1^2 e^{\theta_2}) e^{\theta_1 + \theta_2},$$

$$G(x, t) = (1 + e^{\theta_1} + e^{\theta_2} + a^2 e^{\theta_1 + \theta_2})^2,$$

where  $\theta_1 = k_1 x - k_1^3 t + x_1$ ,  $\theta_2 = k_2 x - k_2^3 t + x_2$ ,  $a = (k_1 - k_2)/(k_1 + k_2)$ ,  $k_1 = 0.4$ ,  $k_2 = 0.6$ ,  $x_1 = 4$ ,  $x_2 = 15$ ,  $a = 1/5$ . In the following simulation, we choose  $\varepsilon = 1$ ,  $\mu = 4.84 \times 10^{-4}$ ,  $\tau = 0.01$  and  $h = 0.02$ .

Figure 3 (a) presents the wave profile of the numerical solution to the Scheme 2 from  $t = 0$  to  $t = 6$ . As is shown in the Figure 3 (b), the Scheme 2 can precisely conserve discrete mass and energy to machine precision. Besides, the wave profile at different times are displayed in Figures 4–6. Compared with the exact wave profile, we can clearly see that the wave shapes of the Scheme 1 and Scheme 2 are captured very well. Specifically, at  $t = 0$ , the taller wave located at the left of the shorter one. However, because the taller wave is faster than the shorter one, it is noted that the taller wave gradually catches up the shorter one at  $t = 2.5$  and occurs interaction at  $t = 3$ . Then, at  $t = 3.5$ , the taller one pass through the shorter wave and continues to travel forward. The  $L_\infty$  errors of the numerical solutions of the proposed schemes are presented in Figure 7, which shows that the numerical errors of the Scheme 1 and Scheme 2 are much the same over  $t \in [0, 6]$ .

### C. Numerical Comparisons

In this example, we consider the following solitary wave,

$$u(x, 0) = 3 \operatorname{sech}^2(0.5x), \quad x \in [-25, 25],$$

under the periodic boundary conditions. Other discretization parameters are set as  $h = 1/3$ ,  $\tau = 0.02$  and  $T = 100$ . Then, the Scheme 1 and Scheme 2 are tested under standard sixth-order central difference operator (i.e., C6) and the compact finite difference operator (i.e., T6). Since the proposed schemes are  $\mathcal{O}(\tau^2)$ , we also consider applying the third-order Heun method and standard fourth-order Runge-Kutta method (RK4) to the following ordinary differential equations,

$$\frac{dU}{dt} = -U * \delta_c^{(1)} U - \delta_c^{(1)} \delta_c^{(2)} U, \quad (19)$$

where  $U = (u_0(t), u_1(t), \dots, u_N(t))^T$  is the semi-discretization of  $u(x, t)$ , and the symbol  $*$  denotes the element-wise product.  $\delta_c^{(1)}$  and  $\delta_c^{(2)}$  represent the C6 or T6 approximation. Concretely, we will consider the following cases,

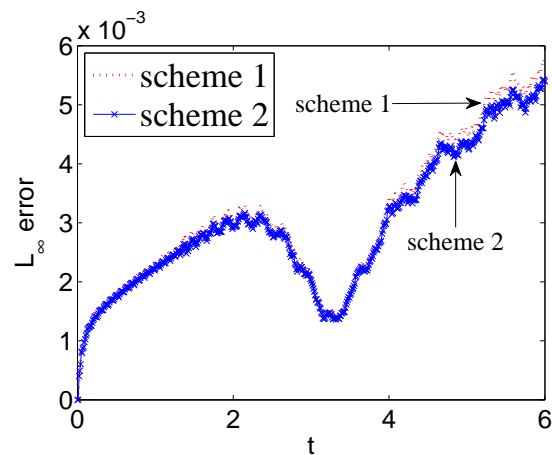


Fig. 7: The  $L_\infty$  errors of the proposed schemes with  $h = 0.02$ ,  $\tau = 0.01$ .

TABLE I: Spatial errors and convergence order of the Scheme 1 with  $\tau = 1 \times 10^{-6}$ ,  $t = 0.0001$ .

$h$	$L_2$	order	$L_\infty$	order	CPU(s)
1/2	$5.3421 \times 10^{-7}$	—	$4.8510 \times 10^{-7}$	—	2.2776
1/4	$6.6602 \times 10^{-9}$	6.33	$6.1133 \times 10^{-9}$	6.31	4.3368
1/8	$9.7235 \times 10^{-11}$	6.09	$9.3875 \times 10^{-11}$	6.03	15.7717
1/16	$1.8866 \times 10^{-12}$	5.69	$2.2990 \times 10^{-12}$	5.35	84.9269

TABLE II: Spatial errors and convergence order of the Scheme 2 with  $\tau = 1 \times 10^{-6}$ ,  $t = 0.0001$ .

$h$	$L_2$	order	$L_\infty$	order	CPU(s)
1/2	$1.1733 \times 10^{-7}$	—	$1.0492 \times 10^{-7}$	—	2.4648
1/4	$1.7919 \times 10^{-9}$	6.03	$1.6189 \times 10^{-9}$	6.02	3.9936
1/8	$2.7225 \times 10^{-11}$	6.04	$2.6163 \times 10^{-11}$	5.95	14.5081
1/16	$4.2268 \times 10^{-13}$	6.01	$4.1878 \times 10^{-13}$	5.97	74.7557

TABLE III: Temporal errors and convergence order of the Scheme 1 with  $h = 1/16$ ,  $t = 1$ .

$\tau$	$L_2$	order	$L_\infty$	order	CPU(s)
1/5	$4.6746 \times 10^{-2}$	—	$2.5880 \times 10^{-2}$	—	20.3269
1/10	$1.0778 \times 10^{-2}$	2.12	$7.1528 \times 10^{-3}$	1.86	35.7398
1/20	$2.7369 \times 10^{-3}$	1.98	$1.7664 \times 10^{-3}$	2.02	62.0884
1/40	$6.9162 \times 10^{-4}$	1.98	$4.4291 \times 10^{-4}$	1.99	104.4271

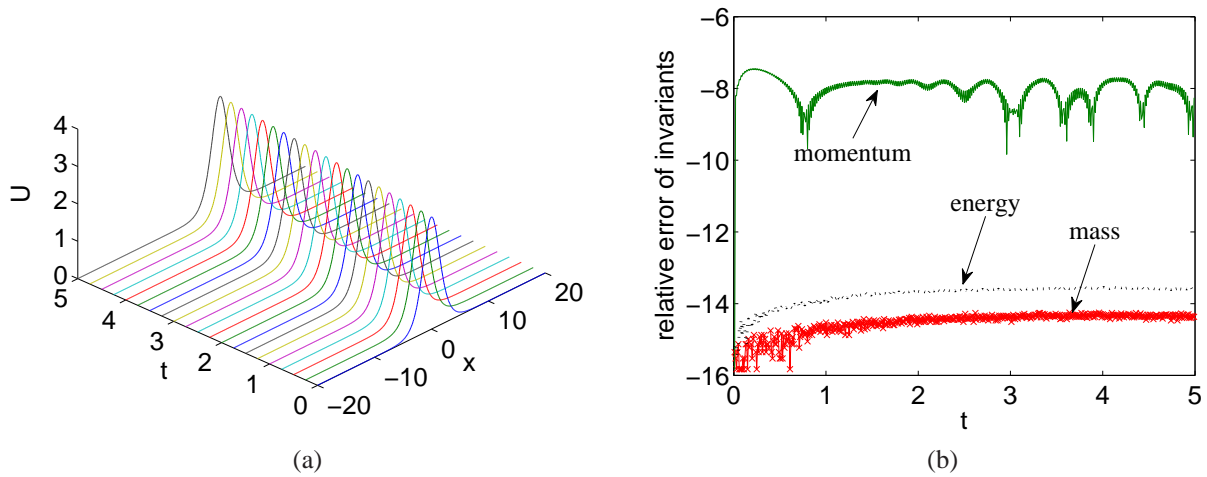


Fig. 1: The numerical results of the Scheme 1 with  $h = 0.1$ ,  $\tau = 0.01$ . (a) numerical solution, (b) the relative errors of invariants.

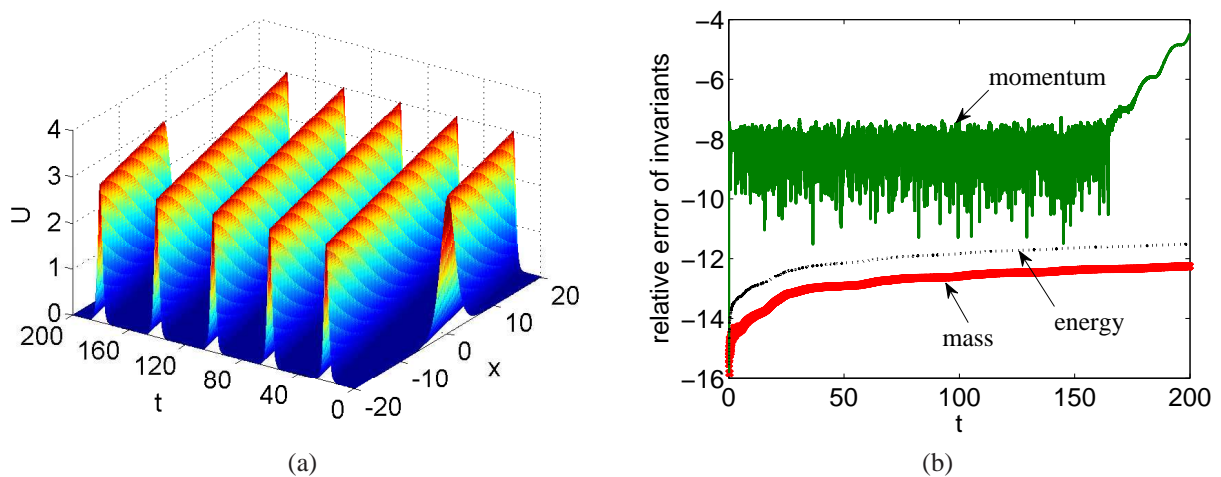


Fig. 2: The numerical results of the Scheme 1 with  $h = 0.1$ ,  $\tau = 0.01$ . (a) numerical solution, (b) the relative errors of invariants.

- Heun method applied to (19) with (C6) as  $\delta_c^{(1)}$  and  $\delta_c^{(2)}$ ,
- Heun method applied to (19) with (T6) as  $\delta_c^{(1)}$  and  $\delta_c^{(2)}$ ,
- RK4 method applied to (19) with (C6) as  $\delta_c^{(1)}$  and  $\delta_c^{(2)}$ ,
- RK4 method applied to (19) with (T6) as  $\delta_c^{(1)}$  and  $\delta_c^{(2)}$ ,
- Scheme 1 (10) with (C6),
- Scheme 1 (10) with (T6),

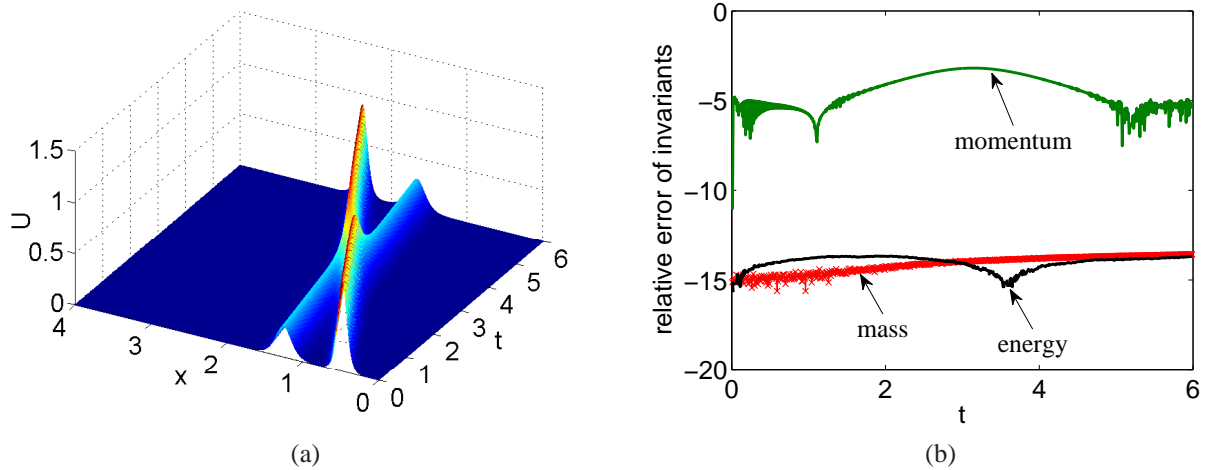


Fig. 3: The numerical results of the Scheme 2 with  $h = 0.02$ ,  $\tau = 0.01$ . (a) numerical solution, (b) the relative errors of invariants.

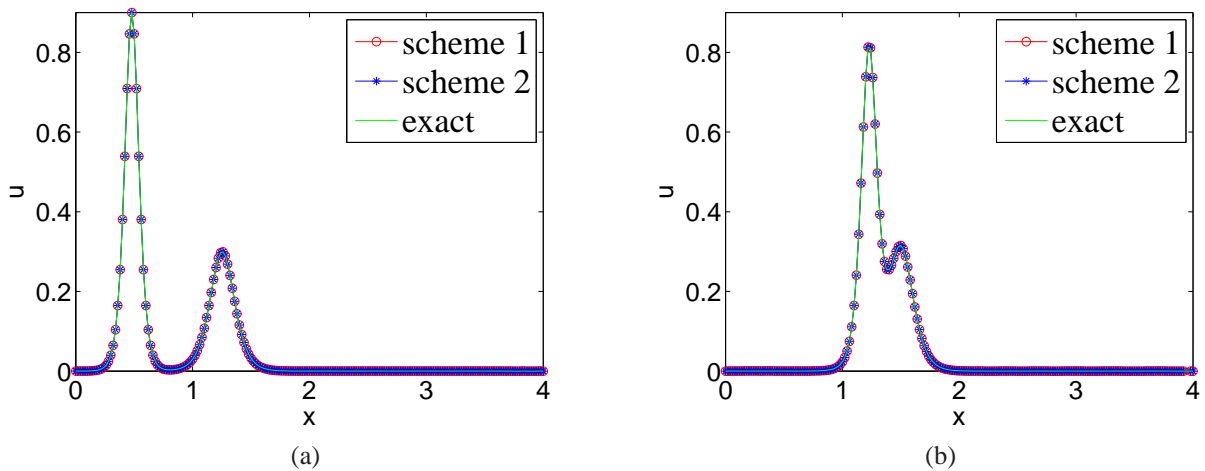


Fig. 4: The numerical solutions computed by the Scheme 1 and Scheme 2 with  $h = 0.02$ ,  $\tau = 0.01$ . (a)  $t = 0$ , (b)  $t = 2.5$ .

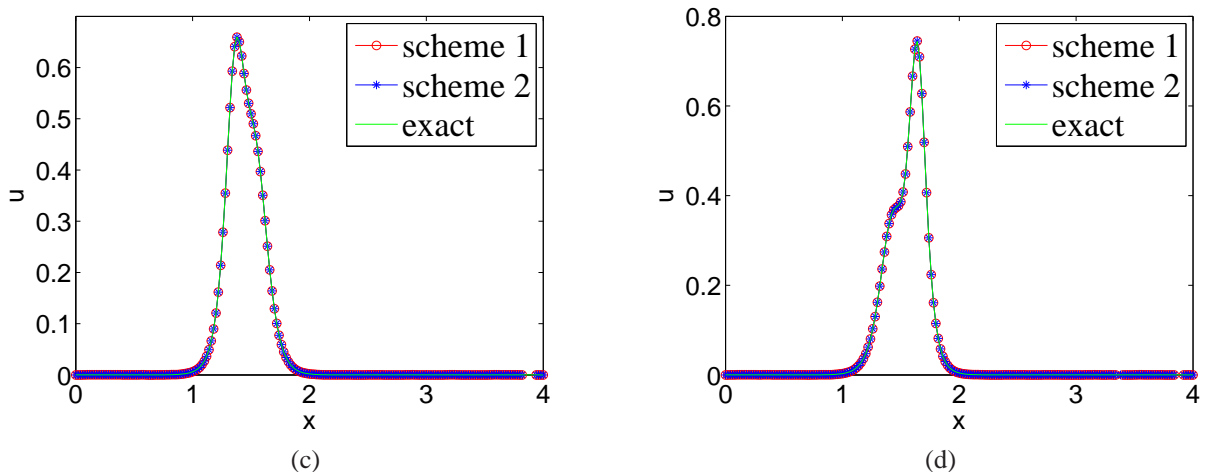


Fig. 5: The numerical solutions computed by the Scheme 1 and Scheme 2 with  $h = 0.02$ ,  $\tau = 0.01$ . (c)  $t = 3$ , (d)  $t = 3.5$ .

- Scheme 2 (14) with (C6),
- Scheme 2 (14) with (T6),

The last four schemes are conservative according to the aforementioned theory.

Figure 8 presents the wave profiles of the numerical solutions obtained by the aforementioned schemes. It is clearly seen that the schemes Heun+(C6), Heun+(T6), RK4+(C6) and RK4+(T6) are unstable, and the Scheme 1 and Scheme 2 provide satisfactory solutions. The evolutions of the discrete

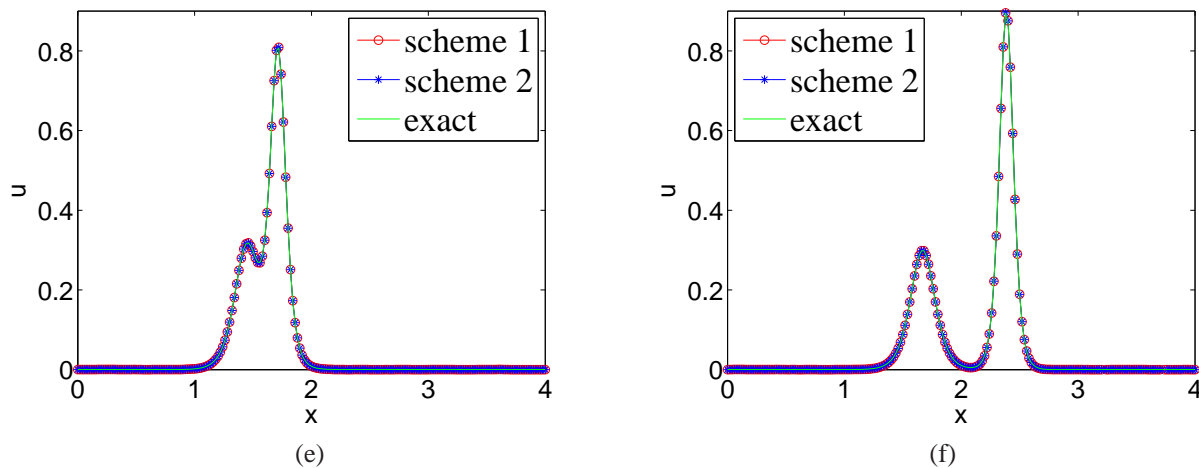


Fig. 6: The numerical solutions computed by the Scheme 1 and Scheme 2 with  $h = 0.02$ ,  $\tau = 0.01$ . (e)  $t = 3.75$ , (f)  $t = 6$ .

energy produced by eight different methods are displayed in Figure 9, which shows that the discrete energy of the schemes Heun+(C6), Heun+(T6), RK4+(C6) and RK4+(T6) are rapidly diverge, which agree with the instability of the solution. In contrast, the Scheme 1 and Scheme 2 can precisely conserve the discrete energy. It indicates that the Scheme 1 and Scheme 2 are superior than the Heun method and RK4 method. Tables IV and V lists the discrete mass and energy at  $t = 100$ . It is clearly seen that the proposed methods can precisely conserve the discrete mass and energy, while the Heun method and RK4 method only conserve the discrete mass.

At last, we compare the aforementioned two spatial discretization technique, i.e., (C6) and (T6), to see if the compact finite difference operator is more accurate than the central difference operator. To this end, we take  $h = 1$ ,  $\tau = 0.02$  and computation domain  $[-50, 50]$ . Figure 10 displayed the magnified detail of the solitary wave solutions obtained by the proposed schemes in both cases of (C6) and (T6), around  $u = 0$  at  $t = 10$ . It is clearly seen that the solution obtained by Scheme 1+C6 produces larger oscillation than the Scheme 1+T6. This result is also hold for the Scheme 2. This may be attributed to the fact that the

central finite difference method can not preserve the correct dispersion relation [19]. Thus, we conclude that the compact finite difference method is more accurate than the central difference operator.

### VI. CONCLUSIONS

In this paper, we propose two linear energy-preserving schemes to solve the KdV equation. The methods are based on the discrete variational derivative method and the sixth-order compact finite difference method. The results show that the proposed schemes can be used to simulate various wave phenomena, and can exactly conserve the discrete mass and energy. Besides, the numerical results also indicate that the energy-preserving compact finite difference schemes are superior to the nonconservative methods in terms of accuracy and stability.

### REFERENCES

- [1] R. M. Miura, C. S. Gardner, and M. D. Kruskal, "Korteweg-de Vries equation and generalisation. II. Existence of conservation laws and constants of motion," *Journal of Mathematical Physics*, vol. 9(8), pp. 1204–1209, 1968.
- [2] H. L. Liu and N. Y. Yi, "A Hamiltonian preserving discontinuous Galerkin method for the generalized Korteweg-de Vries equation," *Journal of Computational Physics*, vol. 321, pp. 776–796, 2016.
- [3] D. Furihata, "Finite difference schemes for  $\frac{\partial u}{\partial t} = \left(\frac{\partial}{\partial x}\right)^\alpha \frac{\partial u}{\partial x}$  that inherit energy conservation or dissipation property," *Journal of Computational Physics*, vol. 156, pp. 181–205, 1999.
- [4] J. Li and M. R. Visbal, "High-order compact schemes for nonlinear dispersive waves," *Journal of Scientific Computing*, vol. 26, pp. 1–23, 2006.
- [5] R. Winther, "A conservative finite element method for the Korteweg-de Vries equation," *Mathematics of Computation*, vol. 34, pp. 23–43, 1980.
- [6] J. Shen, "A new dual-Petrov-Galerkin method for third and higher odd-order differential equations: application to the KdV equation," *SIAM Journal on Numerical Analysis*, vol. 41, pp. 1595–1619, 2004.
- [7] B. Y. Guo and J. Shen, "On spectral approximations using modified legendre rational functions: Application to the Korteweg-de Vries equation on the half line," *Indiana University Mathematics Journal*, vol. 50(1), pp. 181–204, 2001.
- [8] H. Holden, K. H. Karlson, and N. H. Risebro, "Operator splitting methods for generalized Korteweg-de Vries equations," *Journal of Computational Physics*, vol. 153, pp. 203–222, 1999.
- [9] P. F. Zhao and M. Z. Qin, "Multisymplectic geometry and multisymplectic pressmann scheme for the KdV equation," *Journal of Physics A-Mathematical and General*, vol. 33, pp. 3613–3626, 2000.
- [10] Y. Gong, J. Cai, and Y. Wang, "Some new structure-preserving algorithms for general multi-symplectic formulations of Hamiltonian PDEs," *J. Comput. Phys.*, vol. 279, pp. 80–102, 2014.

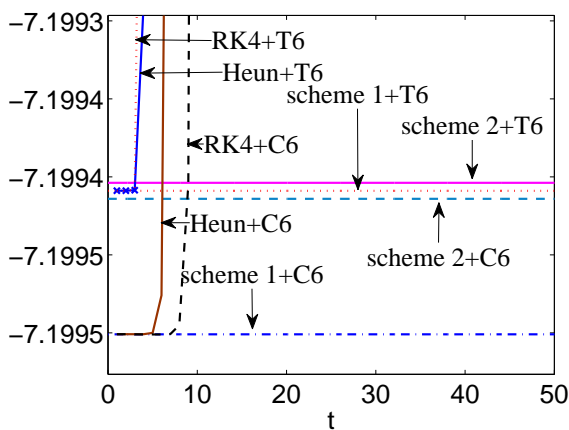


Fig. 9: The discrete energy of different methods with  $h = 1/3$ ,  $\tau = 0.02$ .

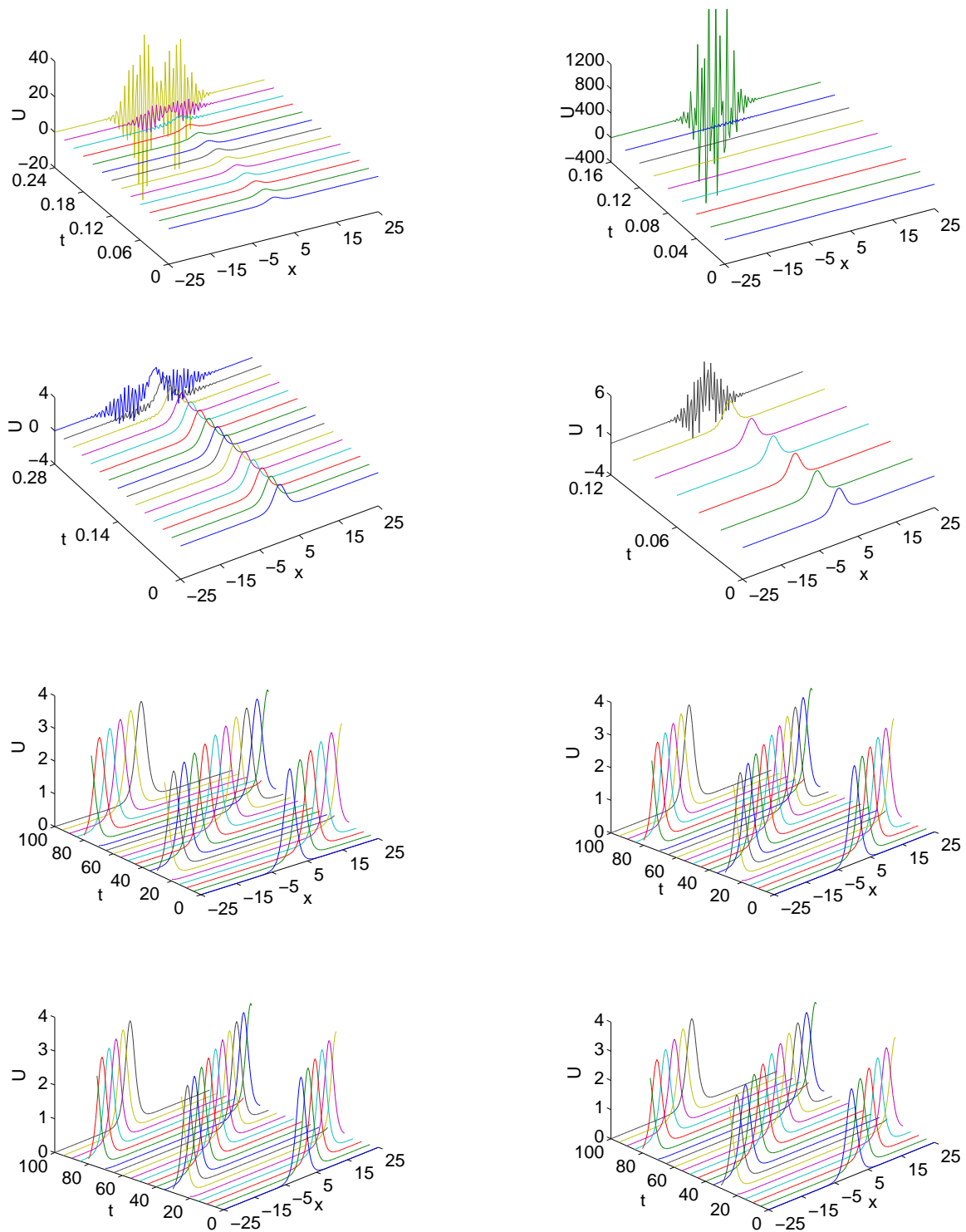


Fig. 8: Numerical solutions computed by different methods with  $h = 1/3$ ,  $\tau = 0.02$ . (top left) Heun+(C6), (top right) Heun+(T6), (2nd left) RK4+(C6), (2nd right) RK4+(T6), (3rd left) Scheme 1+(C6), (3rd right) Scheme 1+(T6), (bottom left) Scheme 2+(C6), (bottom right) Scheme 2+(T6).

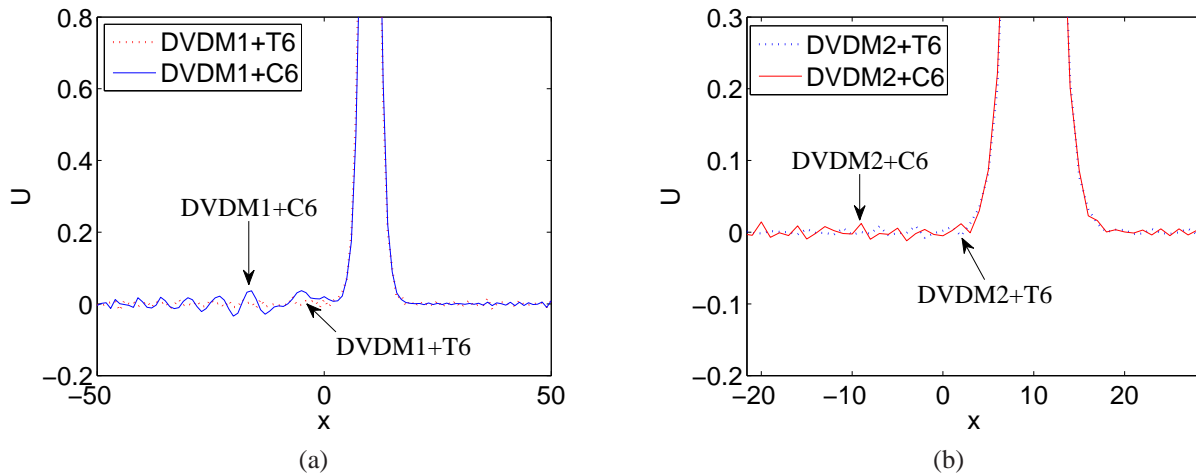


Fig. 10: The numerical solutions computed by the proposed schemes with  $h = 1$ ,  $\tau = 0.02$ . (a) Scheme 1+T6 versus Scheme 1+C6 (b) Scheme 2+T6 versus Scheme 2+C6.

TABLE IV: Maximum and minimum of global mass  $M_d$  and their gap for each scheme at  $t = 100$ .

method	Step sizes	$\max M_d$	$\min M_d$	$ \max M_d - \min M_d $
Scheme 1(C6)	$h = 1/3, \Delta t = 0.01$	11.9999999997198	11.9999999997188	$9.4502 \times 10^{-13}$
Scheme 1(T6)	$h = 1/3, \Delta t = 0.01$	11.9999999997191	11.9999999997190	$1.1369 \times 10^{-13}$
Scheme 2(C6)	$h = 1/3, \Delta t = 0.01$	11.9999999997308	11.9999999997191	$1.1754 \times 10^{-11}$
Scheme 2(T6)	$h = 1/3, \Delta t = 0.01$	11.9999999997195	11.9999999997191	$4.1744 \times 10^{-13}$
Heun (C6)	$h = 1/3, \Delta t = 0.001$	11.9999999997360	11.9999999997191	$1.6954 \times 10^{-11}$
Heun (T6)	$h = 1/3, \Delta t = 0.001$	11.9999999997354	11.9999999997191	$1.6309 \times 10^{-11}$
RK4(C6)	$h = 1/3, \Delta t = 0.01$	11.9999999997360	11.9999999997191	$1.6872 \times 10^{-11}$
RK4(T6)	$h = 1/3, \Delta t = 0.001$	11.9999999997355	11.9999999997191	$1.6412 \times 10^{-11}$

TABLE V: Maximum and minimum of global energy  $H_d$  and their gap for each scheme at  $t = 100$ .

method	Step sizes	$\max H_d$	$\min H_d$	$ \max H_d - \min H_d $
Scheme 1(C6)	$h = 1/3, \Delta t = 0.02$	-7.199550946770	-7.199550946771	$1.4824 \times 10^{-12}$
Scheme 1(T6)	$h = 1/3, \Delta t = 0.02$	-7.199458895279	-7.199458895280	$6.5459 \times 10^{-13}$
Scheme 2(C6)	$h = 1/3, \Delta t = 0.02$	-7.199464066762	-7.199464066783	$2.1535 \times 10^{-11}$
Scheme 2(T6)	$h = 1/3, \Delta t = 0.02$	-7.199453774322	-7.199453774323	$5.1070 \times 10^{-13}$
Heun (C6)	$h = 1/3, \Delta t = 0.001$	-7.200098128216	-7.200098280749	$1.5253 \times 10^{-7}$
Heun (T6)	$h = 1/3, \Delta t = 0.001$	-7.200006063375	-7.200006077933	$1.4558 \times 10^{-8}$
RK4(C6)	$h = 1/3, \Delta t = 0.01$	-7.199962331413	-7.199962535472	$2.0406 \times 10^{-7}$
RK4(T6)	$h = 1/3, \Delta t = 0.001$	-7.200006076954	-7.200006078372	$1.4177 \times 10^{-9}$

[11] N. Y. Yi, Y. Q. Huang, and H. L. Liu, "A direct discontinuous Galerkin method for the generalized Korteweg-de Vries equation: Energy conservation and boundary effect," *Journal of Computational Physics*, vol. 242, pp. 351–366, 2013.

[12] J. L. Bona, H. Chen, O. Karakashian, and Y. Xing, "Conservative, discontinuous-Galerkin methods for the generalized Korteweg-de Vries equation," *Mathematics of computation*, vol. 82(283), pp. 1401–1432, 2013.

[13] J. Yan and L. Zheng, "A class of momentum-preserving Fourier pseudo-spectral schemes for the Korteweg-de Vries equation," *IAENG International Journal of Applied Mathematics*, vol. 49(4), pp. 548–560, 2019.

[14] E. Celledoni, V. Grimm, R. I. McLachlan, D. I. McLaren, D. O'Neale, B. Owren, and G. R. W. Quispel, "Preserving energy resp. dissipation in numerical PDEs, using the "average vector field" method," *Journal of Computational Physics*, vol. 231(20), pp. 6770–6789, 2012.

[15] L. Brugnano, G. Gurioli, "Energy-conserving Hamiltonian boundary value methods for the numerical solution of the Korteweg-de Vries equation," *Journal of Computational and Applied Mathematics*, vol. 351, pp. 117–135, 2019.

[16] D. Furihata and T. Matsuo, *Discrete variational derivative method: a structure-preserving numerical method for partial differential equations*. Boca Raton: CRC press, 2010.

[17] T. Matsuo, "Dissipative or conservative finite-difference schemes for complex-valued nonlinear partial differential equations," *Journal of Computational Physics*, vol. 171, pp. 425–447, 2001.

[18] T. Yaguchi, T. Matsuo, and M. Sugihara, "An extension of the discrete variational method to nonuniform grids," *Journal of Computational Physics*, vol. 229(11), pp. 4382–4423, 2010.

[19] H. Kanazawa, T. Matsuo, and T. Yaguchi, "A conservative compact finite difference scheme for the KdV equation," *Japan Society for Industrial and Applied Mathematics*, vol. 4, pp. 5–8, 2012.

[20] J. Yan and L. Zheng, "New energy-preserving finite volume element scheme for the Korteweg-de Vries equation," *IAENG International Journal of Applied Mathematics*, vol. 47(2), pp. 223–232, 2017.

[21] B. Z. Xu, X. H. Zhang, and D. B. Ji, "A reduced high-order compact finite difference scheme based on POD technique for the two dimensional extended Fisher-Kolmogorov equation," *IAENG International Journal of Applied Mathematics*, vol. 50(3), pp. 474–483, 2020.

[22] X. Zhang, P. Zhang, and Y. Ding, "A reduced high-order compact finite difference scheme based on proper orthogonal decomposition for the generalized Kuramoto-Sivashinsky equation," *IAENG International Journal of Applied Mathematics*, vol. 49(2), pp. 165–174, 2019.

**Jin-liang Yan** was born in Pingyao, Shanxi Province, China, in 1979. The author respectively received his Ph.D. and Master's degrees in computational mathematics at Nanjing Normal University, Nanjing, Jiangsu Province, China, in July 2016 and July 2010. Now, he is an associate professor of the Department of Mathematics and Computer, Wuyi University, Wuyishan, China. His research interests include structure-preserving algorithms, numerical solution of partial differential equations, and computing sciences.

**Liang-hong Zheng** was born in Nanping, Fujian Province, China, in 1983. She received her bachelor's degree in computer science and technology from Minnan Normal University, Zhangzhou, Fujian Province, China, in July 2009.

Presently, she is a lecturer of the Department of Information and Technology, Nanping No. 1 Middle School, Nanping, China. Her research interests include algorithm design, artificial intelligence, robot competition, and video production.

**Fu-qiang Lu** was born in Xinyang, Henan Province, China. He received his Ph.D. and Master's degrees in computational mathematics at Nanjing Normal University, Nanjing, Jiangsu Province, China, in July 2016 and July 2010.

Presently, he is a lecturer of Changzhou Institute of Technology, Changzhou, China. His research interests is numerical solution of partial differential equations.

**Wen-Jun Li** now is an undergraduate student of the Department of Mathematics and Computer, Wuyi University, Wuyishan, China.